Decolorization of Reactive Dye Solutions by Electrocoagulation Using Aluminum Electrodes

3 AUTHORS:

Orhan Taner Can
Bitlis Eren University
21 PUBLICATIONS 1,049 CITATIONS

SEE PROFILE

Mahmut Bayramoğlu
Gebze Technical University
83 PUBLICATIONS 2,654 CITATIONS

SEE PROFILE

Mehmet Kobya
Gebze Technical University
73 PUBLICATIONS 3,652 CITATIONS

SEE PROFILE

3391

Decolorization of Reactive Dye Solutions by Electrocoagulation Using Aluminum Electrodes

O. T. Can, M. Bayramoglu, and M. Kobya*

Engineering Faculty, Department of Environmental Engineering, Gebze Institute of Technology, 41400 Gebze, Turkey

The removal of pollutants from effluents by electrocoagulation has become an attractive method in recent years. This paper deals with the batch removal of the reactive textile dye Remazol Red RB 133 from an aqueous medium by the electrocoagulation method using aluminum electrodes. The effects of wastewater conductivity, initial pH, current density, stirring rate, dye concentration, and treatment time on the decolorization efficiency and energy consumption have been investigated. Aluminum hydroxypolymeric species formed during an earlier stage of the operation efficiently remove dye molecules by precipitation, and in a subsequent stage, $Al(OH)_3$ flocs trap colloidal precipitates and make solid−liquid separation easier during the flotation stage. These stages of electrocoagulation must be optimized to design an economically feasible electrocoagulation process.

1. Introduction

The pollution induced by dyestuff losses and discharge during dying and finishing processes in the textile industry has been a serious environmental problem for years; dyes in the wastewater undergo chemical as well as biological changes, consume dissolved oxygen from the stream, and destroy aquatic life because of their toxicity.[1] It is therefore necessary to treat textile effluents prior to their discharge into the receiving water.

Traditional methods for dealing with textile wastewater consist of various combinations of biological, physical, and chemical methods.[2] Common biological treatment processes are often ineffective in removing dyes which are highly structured polymers with low biodegradability.[3] Various physical−chemical techniques are also available for the treatment of aqueous streams to eliminate dyes; chemical coagulation followed by sedimentation[4] and adsorption are the widely used ones,[5] but other advanced techniques are often applied, e.g., UV,[6,7] ozonation,[8] ultrasonic decomposition, or combined oxidation processes.[9−11] Meanwhile, high treatment costs of these methods have stimulated, in recent years, the search for more cost-effective treatment methods.

Electrocoagulation is a process consisting of creating metallic hydroxide flocs within the wastewater by electrodissolution of soluble anodes, usually made of iron or aluminum. This method has been practiced for most of the 20th century with limited success. Recently, however, there has been renewed interest in the use of electrocoagulation owing to the increase in environmental restrictions on effluent wastewater. In the past decade, this technology has been increasingly used in developed countries for the treatment of industrial wastewaters.[12−14] Electrocoagulation has been proposed for the treatment of various effluents such as wastewater containing food and protein wastes,[15] textile wastewater,[16] aqueous suspensions containing kaolinite, bentonite, and ultrafine particles,[17,18] fluoride-containing water,[19] restaurant wastewater,[20,21] textile dye solutions,[22,23] and smelter wastewater containing harmful arsenic.[24]

The purpose of this study is to conduct an experimental investigation on the removal of a reactive textile dye (Remazol Red RB 133) from the wastewater using the electrocoagulation method. Several fundamental aspects regarding the effects of wastewater conductivity, initial pH, current density, stirring rate, dye concentration, and time on the dye removal efficiency are explored.

2. Electrocoagulation

Generally, three main processes occur during electrocoagulation: (a) electrolytic reactions at electrode surfaces; (b) formation of coagulants in the aqueous phase; (c) adsorption of soluble or colloidal pollutants on coagulants and removal by sedimentation or flotation.

The main reactions at the electrodes are

$$\text{Anode:} \quad Al \rightarrow Al(aq)^{3+} + 3e \tag{1}$$

$$\text{Cathode:} \quad 3H_2O + 3e \rightarrow {}^3/_2H_2 + 3OH^- \tag{2}$$
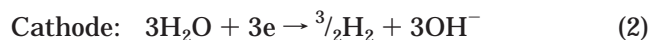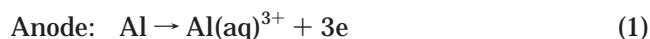
If the anode potential is sufficiently high, secondary reactions may occur also, such as direct oxidation of organic compounds and of Cl^- ions present in wastewater:[20]

$$2Cl^- \rightarrow Cl_2 + 2e \tag{3}$$

The chlorine produced is a strong oxidant that can oxidize some organic compounds.

On the other hand, the cathode may be chemically attacked by OH^- ions generated during H_2 evolution at high pH values:[25]

$$2Al + 6H_2O + 2OH^- \rightarrow 2Al(OH)_4^- + 3H_2 \tag{4}$$
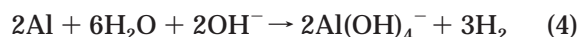
$Al(aq)^{3+}$ and OH^- ions generated by electrode reactions (1) and (2) react to form various monomeric species such

* To whom correspondence should be addressed. Tel.: +90-262-6538457. Fax: +90-262-6538490. E-mail: kobya@gyte.edu.tr.
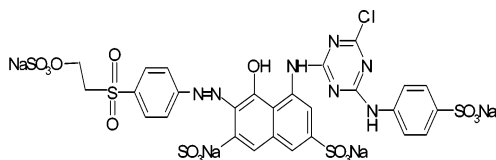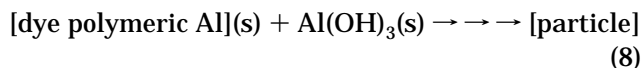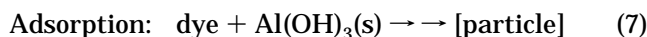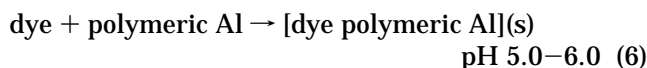
Figure 1. Molecular structure of the reactive dye Remazol Red RB 133.

as $Al(OH)^{2+}$, $Al(OH)_2^+$, $Al_2(OH)_2^{4+}$, and $Al(OH)_4^-$ and polymeric species such as $Al_6(OH)_{15}^{3+}$, $Al_7(OH)_{17}^{4+}$, $Al_8(OH)_{20}^{4+}$, $Al_{13}O_4(OH)_{24}^{7+}$, and $Al_{13}(OH)_{34}^{5+}$, which transform finally into $Al(OH)_3$ according to complex precipitation kinetics.[26,27]

Formation rates of the different species play an important role in the decolorization process. Several interaction mechanisms are possible between dye molecules and hydrolysis products, and the rates of these depend on the pH of the medium and types of ions present. Two major interaction mechanisms have been considered in recent years: precipitation and adsorption, each one being proposed for a separate pH range. Flocculation in the low pH range is explained as precipitation, while that in the higher pH range (>6.5) is explained as adsorption.[25,26]

Precipitation:

$$\text{dye} + \text{monomeric Al} \rightarrow [\text{dye monomeric Al}](s)$$
$$\text{pH } 4.0-5.0 \quad (5)$$

$$\text{dye} + \text{polymeric Al} \rightarrow [\text{dye polymeric Al}](s)$$
$$\text{pH } 5.0-6.0 \quad (6)$$

Adsorption: $$\text{dye} + Al(OH)_3(s) \rightarrow \rightarrow [\text{particle}] \quad (7)$$

$$[\text{dye polymeric Al}](s) + Al(OH)_3(s) \rightarrow \rightarrow \rightarrow [\text{particle}] \quad (8)$$
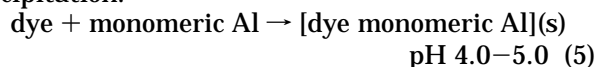
At high pH values above 9, $Al(OH)_4^-$ is also present in the system.

Freshly formed amorphous $Al(OH)_3$ "sweep flocs" have large surface areas, which is beneficial for a rapid adsorption of soluble organic compounds and trapping of colloidal particles. These flocs polymerize as

$$n Al(OH)_3 \rightarrow Al_n(OH)_{3n} \quad (9)$$

and they are removed easily from the aqueous medium by sedimentation and by H_2 flotation.

3. Materials and Methods

3.1. Materials. The commercially available reactive dye Remazol Red RB 133 was obtained from DyStar with a molecular structure as shown in Figure 1. The characteristics of Remazol Red RB 133 were provided by DyStar and are summarized in Table 1.

3.2. Experimental Apparatus. The experimental setup is shown in Figure 2. The thermostated electrocoagulator was made of Plexiglas with the dimensions $65 \times 65 \times 110$ mm. Two anodes and two cathodes with dimensions of $46 \times 55 \times 3$ mm, made of plate aluminum (Al: 99.53%), were connected to a digital dc power supply (Topward 6306D; 30 V and 6 A) in monopolar mode. The total effective electrode area was 78 cm^2, and the spacing between electrodes was 11 mm.

Table 1. Characterization of the Remazol Red RB 133

parameter	value
colour index	Ractive Red RB133
chromophore	Azo
reactive anchor systems	MCT and VS[a]
molar mass (nonhydrolyzed dye)	984.2
percentage of pure dye	63%
water solubility at 293 K (g/L)	70
acute oral totoxicity LD_{50} (mg/kg)	2000
fish toxicity LC_0 (mg/L)	>500
pH value (at 10 g/L water)	7
COD value (mg/g)	540
BOD_5 value (mg/g)	<10
DOC value (mg/g)	120

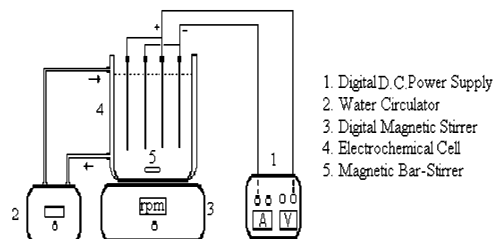[a] Monochlorotriazine (MCT) and vinylsulfone (VS).

Figure 2. Schematic diagram of the experimental setup.

3.3. Experimental Procedure. All of the runs are performed at a constant temperature of 25 °C and at a constant magnetic stirring speed of 200 rpm. In each run, 250 cm^3 of the dye solution was placed into the electrolytic cell. The current density was adjusted to a desired value (galvanostatic mode), and the run was started. At the end of the run, the solution was filtered and the filtrate was centrifuged at 200 rpm. Before each run, organic impurities on electrode surfaces were removed by washing with acetone, while the surface oxide layer was removed by dipping for 5 min in a solution freshly prepared by mixing 100 cm^3 of a HCl solution (35%) and 200 cm^3 of a hexamethylenetetra-amine $[(CH_2)_6N_4]$ aqueous solution (2.80%).[15] At the end of the run, the electrodes were washed thoroughly with water to remove any solid residues on the surfaces, dried, and reweighed.

3.4. Analytical Method. The dye solutions containing Remazol Red RB 133 were prepared in distilled water. The pH and conductivity were adjusted to a desirable value using NaOH or H_2SO_4 and NaCl, respectively.

Samples of dye solutions were analyzed using a Shimadzu model UV-160 double-beam spectrophotometer. Dye concentrations were determined using a working curve by plotting the absorbances versus known concentrations at λ_{max} (518 nm of Remazol Red RB 133).

The decolorization efficiency, E, is calculated as

$$E = \frac{C_i - C_f}{C_i} \times 100 \quad (10)$$

where C_i is the initial dye concentration (mg/L) and C_f the final dye concentration (mg/L).

4. Results and Discussion

The effects of the initial pH, conductivity, stirring rate, current density, treatment time, and dye concen-
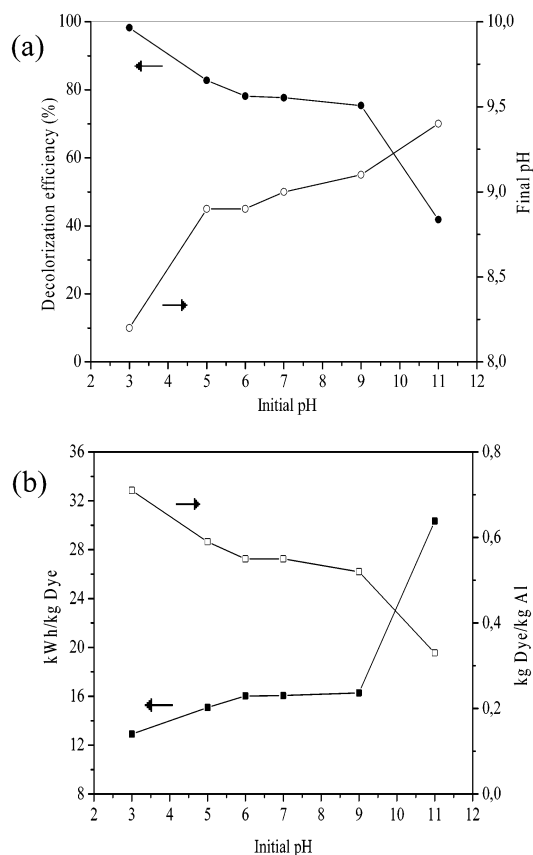
Figure 3. Effect of the initial pH (a) on the decolorization efficiency and (b) on the energy consumption and decolorization capacity (conductivity, 2000 μS/cm; current density, 10 mA/cm^2; dye concentration, 250 mg/L; stirring rate, 200 rpm; treatment time, 10 min).

Figure 4. Effect of conductivity (a) on the decolorization efficiency and (b) on the energy consumption and decolorization capacity (current density, 10 mA/cm^2; dye concentration, 250 mg/L; stirring rate, 200 rpm; initial pH, 6; time, 10 min).

tration are investigated on three process responses: decolorization efficiency, decolorization capacity (kilograms of dye removed per kilograms of total dissolved Al), and electrical energy consumption (kilowatt hour per kilogram of dye removed).

4.1. Effect of the Initial pH. The effect of pH is investigated between 3 and 11. According to the electrode reactions (1) and (2), Al^{3+} and OH$^-$ ions are generated in the molar ratio 1:3; meanwhile, for the polymeric species precipitating at pH 5–6, this ratio is less than 3, between 2 and 2.5. This means that the OH$^-$ ion accumulates in the aqueous phase during the process, and its concentration is dictated not only by the initial pH but also by the reaction kinetics and equilibria occurring in this complicated aqueous system. As seen in Figure 3a, by increasing the initial pH from 3 to 9, the final pH increases approximately from 8 to nearly 9, where it remains almost constant because of the buffering capacity of the system Al(OH)$_3$/Al(OH)$_4^-$, which decreases the final pH from high values down to 9.4 by consuming OH$^-$ according to reaction (11).

$$Al(OH)_3 + OH^- \Leftrightarrow Al(OH)_4^- \qquad (11)$$

A low initial pH retards the formation of Al(OH)$_3$ flocs and stimulates the formation of hydroxypolymeric species; as seen in Figure 3a, high efficiencies obtained with low initial pH values, e.g., 3, result from an efficient precipitation of dye molecules, according to the mechanism outlined by eqs 5 and 6. The decolorization efficiency shows a constant plateau for the initial pH
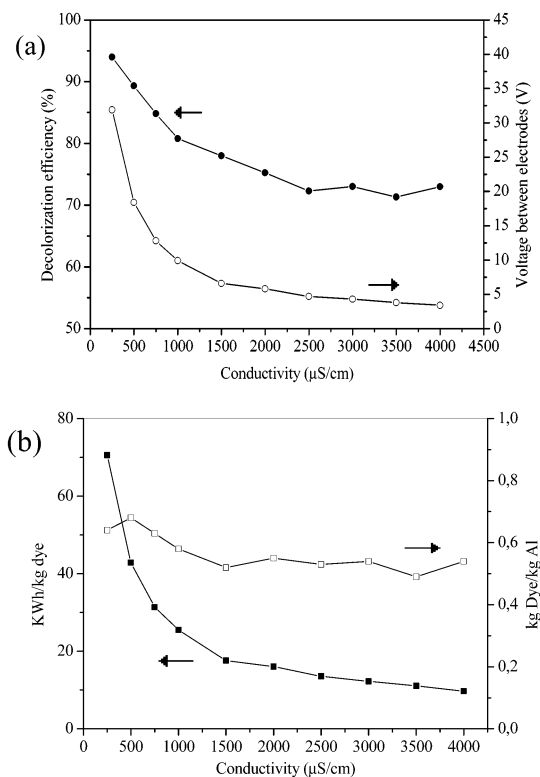
between 5 and 9 and then falls again for higher pH values. The decolorization capacity, as seen in Figure 3b, exhibits the same trends. As found by electrode weight measurements, the initial pH has a negligible effect on the total masses of dissolved electrodes. This suggests that the dye precipitation process is primarily responsible of the high decolorization efficiency, and adsorption of the dye polymeric species colloidal precipitates by Al(OH)$_3$ flocs has a more secondary effect. Moreover, it is clear that, especially at high pH values above 9, the quantity of flocs diminishes according to eq 11; thus, the decolorization efficiency and capacity fall.

Finally, the electrical energy consumed per kilogram of dye removed, as seen in Figure 3b, is also dependent on the initial pH; an acidic or neutral initial medium is beneficial for low electrical energy consumption. The sudden increase of energy consumption above pH 9 is due to the same causes diminishing decolorization performances.

4.2. Effect of Conductivity. The effect of conductivity is investigated between 250 and 4000 μS/cm by using NaCl as the supporting electrolyte. As seen in Figure 4a, the decolorization efficiency decreases steadily as the conductivity increases. The final pH of the medium and the mass of dissolved anodes are almost independent of the varying conductivity. Thus, the decrease in the decolorization efficiency with increasing conductivity may not be attributed to these factors, but it may be attributed to a change in the ionic strength due to changing conductivity of the aqueous medium. Ionic strength affects clearly the kinetics and equilibria of reactions between charged species occurring during electrocoagulation.
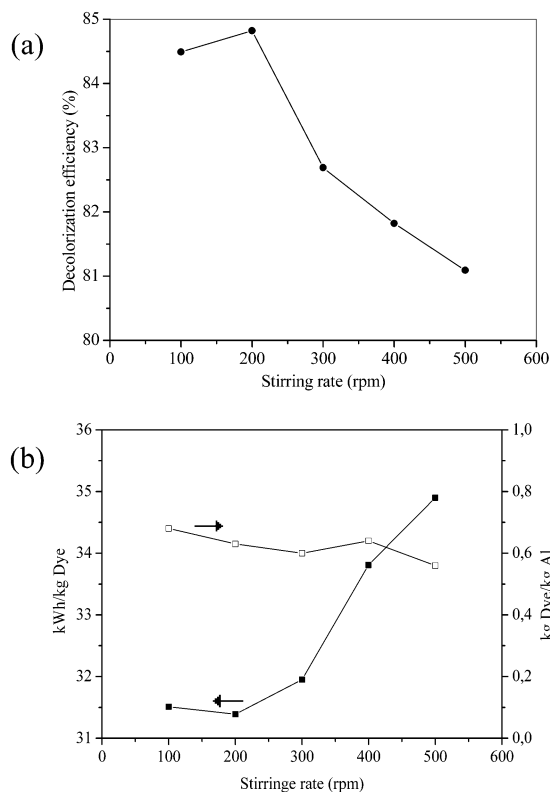
(a)

(b)

Figure 5. Effect of the stirring rate (a) on the decolorization efficiency and (b) on the energy consumption and decolorization capacity (current density, 10 mA/cm^2; dye concentration, 250 mg/L; conductivity, 750 μS/cm; initial pH, 6; time, 10 min).

(a)

(b)

Figure 6. Effect of the current density (a) on the decolorization efficiency and (b) on the energy consumption and decolorization capacity (dye concentration, 250 mg/L; conductivity, 750 μS/cm; initial pH, 6; time, 10 min).

On the other hand, the decolorization capacity shows a weak peak at the conductivity 500 μS/cm and then decreases steadily, as seen also in Figure 4a. The cell voltage and energy consumption decrease, as expected, with increasing conductivity, as seen in Figure 4b.

4.3. Effect of the Stirring Rate. The stirring rate is varied between 100 and 500 rpm to investigate its effect on the process performance. As seen in Figure 5a, the decolorization efficiency shows a maximum for 200 rpm and then it decreases smoothly. The maximum point may be explained by the favorable effect of the stirring rate on mass transfer, and the decrease in efficiency at higher stirring rates may be due to the destabilization of Al(OH)$_3$ flocs. The final pH is unaffected by the stirring rate. Small increases are observed on the anodic and cathodic dissolutions; meanwhile, the decolorization capacity shows an inverse trend and decreases slightly (Figure 5a). On the other hand, the cell voltage and energy consumption exhibit small increases with increasing stirring rate, as shown in Figure 5b.

4.4. Effect of the Current Density and Time. The current density is varied between 2.5 and 25 mA/cm^2 to determine its effect on the process performance of the electrocoagulator. The decolorization efficiency increases rapidly up to 92.50% with a current density of 15 mA/cm^2, and then it remains almost constant for higher current densities, as depicted in Figure 6a, where it is also seen that the decolorization capacity is inversely proportional to the current density. The final pH is nearly constant at 9; thus, it is unaffected by the current density. Dissolved amounts of both anodes and cathodes are fairly linearly dependent on the current density.

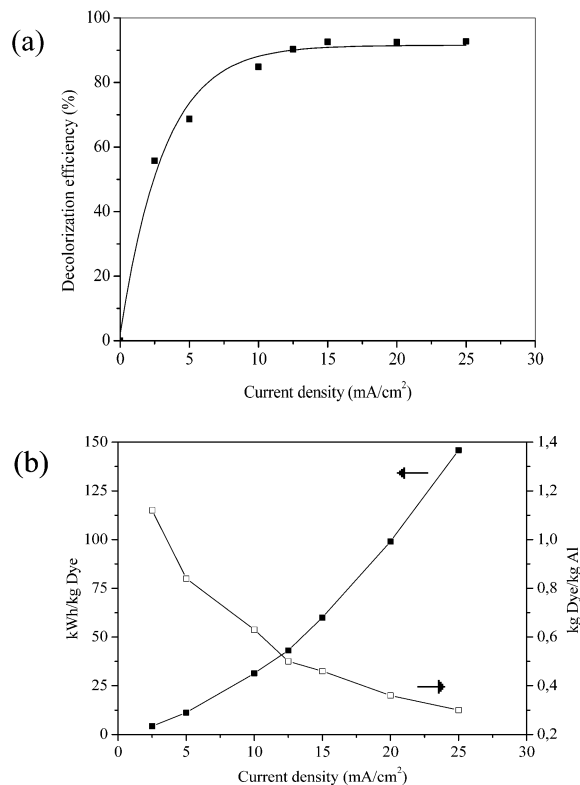If a linear regression is applied between log(decolori-

zation efficiency) and log(M_T), where M_T is the total dissolved amount of Al electrodes, a high correlation coefficient ($r^2 = 0.95$) is obtained with the following relation:

$$\text{decolorization efficiency} \propto M_T^{0.70} \qquad (12)$$

and

$$\text{decolorization capacity} \propto M_T^{-0.63} \qquad (13)$$

The same relationship is also observed for some chemical adsorbents.[28] These relationships indicate that a limited amount of dissolved electrodes participates in the formation of hydroxypolymeric species, and also the enmeshing capacity of flocs is not linearly related to the flocs mass.

As seen in Figure 6b, the voltage is a linear function of the current density, as expected. Approximately a 35-fold increase in the energy consumption occurs, when the current density is increased 10-fold.

Similar conclusions may be drawn for the effect of the treatment time when parts a and b of Figure 7 are compared with parts a and b of Figure 6. The decrease in the decolorization capacity when time progresses, as seen in Figure 7a, reflects the progressive formation of surplus flocs. The similarity between the effects of the treatment time and the current density suggests to combine these two parameters into one parameter, namely, the quantity of electricity consumed per cubic meter of effluent, expressed as faradays per cubic meter. To test this suggestion, the decolorization efficiency is plotted as a function of this new parameter in Figure 8; data points obtained separately, with time and current density as parameters, fall nearly on the same
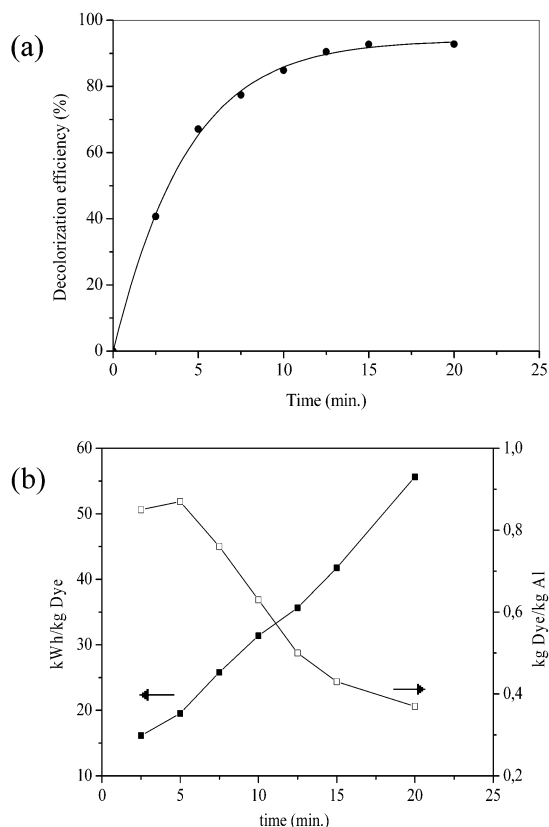
Figure 7. Effect of time (a) on the decolorization efficiency and (b) on the energy consumption and decolorization capacity (dye concentration, 250 mg/L; conductivity, 750 μS/cm; initial pH, 6; current density, 10 mA/cm^2).
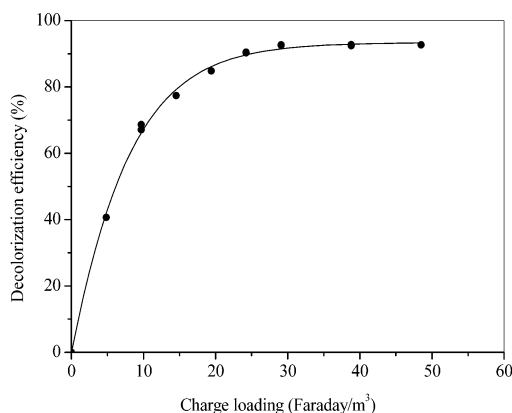

Figure 8. Effect of charge loading on the decolorization efficiency (dye concentration, 250 mg/L; conductivity, 750 μS/cm; initial pH, 6).

plot. A linear regression between log(efficiency) and log-(faradays/m^3) yields the following relation:

$$\text{decolorization efficiency} \propto (\text{faradays/m}^3)^{0.30}$$
$$(r^2 = 0.994) \quad (14)$$

4.5. Effect of the Dye Concentration. The decolorization efficiency falls from 100% to 70% when the dye concentration is increased from 100 to 1000 mg/L, which means that the efficiency is a function of the dye concentration, as seen in Figure 8a. The final pH of the dye solution and the mass of dissolved aluminum anodes are nearly independent of the dye concentration. Meanwhile, the decolorization capacity, as seen also in Figure 9a, is a function of the dye concentration. When log-
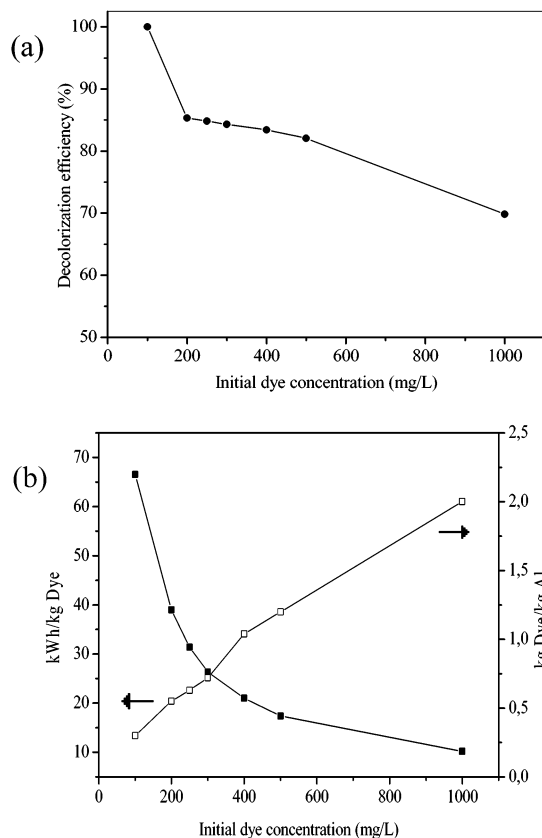

Figure 9. Effect of the initial dye concentration (a) on the decolorization efficiency and (b) on the energy consumption and decolorization capacity (time, 10 min; conductivity, 750 μS/cm; initial pH, 6; current density, 10 mA/cm^2).

(decolorization capacity) is regressed to log(dye concentration), the following relationship is obtained, with $r^2 = 0.986$:

$$\text{decolorization capacity} \propto C_0^{-0.16} \quad (15)$$

Relationship (15) is typical for chemical coagulants with a Freundlich-type adsorption isotherm.

Finally, the cell voltage increases slightly with increasing dye concentration. Despite the small increase in the cell voltage at a constant current density, the energy consumption shows a strong inverse relationship with the dye concentration, as seen in Figure 9b.

5. Conclusion

Electrocoagulation is an efficient process to remove dye from effluent wastewater. The initial pH of the dye solution and the quantity of electricity consumed (faradays/m^3) are important process variables that affect the process decolorization efficiency, as well as the process economics via variable cost items such as electrical energy and electrode material consumption. The process conditions must be optimized to obtain large quantities of polymeric species that rapidly precipitate dye molecules and an optimum amount of Al(OH)$_3$ flocs that efficiently trap colloidal precipitates and make solid–liquid separation easier during the flotation phase.

Literature Cited

(1) Ahmed, M. N.; Ram, R. N. Removal of basic dye from wastewater using silica as adsorbent. *Environ. Pollut.* **1992**, *77*, 79−85.

(2) Abo-Elela, S. I.; El-Gohary, F. A.; Ali, H. L.; Abdel-Wahaab, R. S. Treatability studies of textile wastewater. *Environ. Technol. Lett.* **1988**, *9*, 101−109.

(3) Lin, S. H.; Chen, M. L. Treatment of textile wastewater by chemical methods for reuse. *Water Res.* **1997**, *31*, 868−876.

(4) Lin, S. H.; Lin, C. M. Treatment of textile waste effluents by ozonation and chemical coagulation. *Water Res.* **1993**, *27*, 1743−1748.

(5) McKay, G. Color removal by adsorption. *Am. Dyest. Rep.* **1990**, *69*, 38−51.

(6) Arslan, I.; Akmehmet Balcioglu, I. Degradation of commercial reactive dyestuffs by heterogenous and homogenous advanced oxidation processes: a comparative study. *Dyes Pigm.* **1999**, *43*, 95−108.

(7) Hachem, C.; Bocquillon, F.; Zahraa, O.; Bouchy, M. Decolourization of textile industry wastewater by the photocatalytic degradation process. *Dyes Pigm.* **2001**, *49*, 117−125.

(8) Liakou, S.; Pavlou, S.; Lyberatos, G. Ozonation of azo dyes. *Water Sci. Technol.* **1997**, *35*, 279−286.

(9) Arslan, I.; Balcioglu, I. A.; Tuhkanen, T. Advanced oxidation of synthetic dyehouse effluent by O_3, H_2O_2/O_3 and H_2O_2/UV processes. *Environ. Technol.* **1999**, *20*, 921−931.

(10) Lorimer, J. P.; Mason, T. J.; Plattes, M.; Phull, S. S. Dye effluent decolourization using ultrasonically assisted electro-oxidation. *Ultrason. Sonochem.* **2000**, *7*, 237−242.

(11) Fung, P. C.; Huang, S. M.; Tsui, S. M.; Poon, C. S. Treatability study of organic and colour removal in desizing/dyeing wastewater by UV/US system combined with hydrogen peroxide. *Water Sci. Technol.* **1999**, *40*, 153−160.

(12) Scott, K. *Electrochemical Processes for Clean Technology*; University of Newcastle upon Tyne: London, 1995.

(13) Rajeshwar, K.; Ibanez, J. G.; Swain, G. M. Electrochemistry and the environment. *J. Appl. Electrochem.* **1994**, *24*, 1077−1091.

(14) Mollah, M. Y. A.; Schennach, R.; Parga, J. P.; Cocke, D. L. Electrocoagulation (EC)−science and applications. *J. Hazard. Mater.* **2001**, *B84*, 29−41.

(15) Do, J. S.; Chen, M. L. Decolourization of dye-containing solutions by electrocoagulation. *J. Appl. Electrochem.* **1994**, *24*, 785−790.

(16) Lin, S. H.; Peng, C. F. Treatment of textile wastewater by electrochemical method. *Water Res.* **1994**, *28*, 277−282.

(17) Matteson, M. J.; Dobson, R. L.; Glenn, R. W., Jr.; Kukunoor, N. S.; Waits, W. H., III.; Clayfield, E. J. Electrocoagulation and separation of aqueous suspensions of ultrafine particles. *Colloids Surf. A* **1995**, *104*, 101−109.

(18) Donini, J. C.; Kan, J.; Szynkarczuk, J.; Hassan, T. A.; Kar, K. L. Operating cost of electrocoagulation. *Can. J. Chem. Eng.* **1994**, *72*, 1007−1012.

(19) Mameri, N.; Lounici, H.; Belhocine, D.; Grib, H.; Piron, D. L.; Yahiat, Y. Defluoridation of Shara water by small plant electrocoagulation using bipolar aluminium electrodes. *Sep. Purif. Technol.* **2001**, *24*, 113−119.

(20) Chen, X.; Chen, G.; Yue, P. L. Separation of pollutants from restaurant wastewater by electrocoagulation. *Sep. Purif. Technol.* **2000**, *19*, 65−76.

(21) Chen, G.; Chen, X.; Yue, P. L. Electrocoagulation and electroflotation of restaurant wastewater. *J. Environ. Eng.* **2000**, *126*, 858−863.

(22) Öğütveren, Ü. B.; Gönen, N.; Koparal, S. Removal of dye stuffs from wastewater: electrocoagulation and acilan blau using soluble anode. *J. Environ. Sci. Health* **1992**, *A27*, 1237−1247.

(23) Xiong, Y.; Strunk, P. J.; Xia, H.; Zhu, X.; Karlsson, H. T. Treatment of dye wastewater containing acid orange II using a cell with three-phase three-dimensional electrode. *Water Res.* **2001**, *35*, 4226−4230.

(24) Balasubramanian, N.; Madhavan, K. Arsenic removal from industrial effluent through electrocoagulation. *Chem. Eng. Technol.* **2001**, *24*, 519−521.

(25) Picard, T.; Cathalifaund-Feuillade, G.; Mazet, M.; Vandensteendam, C. Cathodic dissolution in the electrocoagulation process using aluminium electrodes. *J. Environ. Monit.* **2000**, *2*, 77−80.

(26) Gürses, G.; Yalcin, M.; Dogan, C. Electrocoagulation of some reactive dyes: a stastical investigation of some electrochemical variables. *Waste Manage.* **2002**, *22*, 491−499.

(27) Rebhun, M.; Lurie, M. Control of organic matter by coagulation and floc separation. *Water Sci. Technol.* **1993**, *27*, 1−20.

(28) Sharma, D. C.; Forster, C. F. The treatment of chromium wastewaters using the sorptive potential of leaf mould. *Bioresour. Technol.* **1994**, *49*, 31−40.